Article

Hemp Fiber-Modified Asphalt Concretes with Reclaimed Asphalt Pavement for Low-Traffic Roads

Apinun Buritatum [1,2], Apichat Suddeepong [1,2,*], Kongsak Akkharawongwhatthana [1], Suksun Horpibulsuk [1,2,3,4,5], Teerasak Yaowarat [1,2], Menglim Hoy [1,3], Arul Arulrajah [6] and Ahmad Safuan A. Rashid [4]

[1] Center of Excellence in Innovation for Sustainable Infrastructure Development, Suranaree University of Technology, Nakhon Ratchasima 30000, Thailand
[2] School of Civil and Infrastructure Engineering, Suranaree University of Technology, Nakhon Ratchasima 30000, Thailand
[3] School of Civil Engineering, Suranaree University of Technology, Nakhon Ratchasima 30000, Thailand
[4] Department of Geotechnics and Transportation, Universiti Teknologi Malaysia, Johor Bahru 81310, Malaysia
[5] Academy of Science, The Royal Society of Thailand, Bangkok 10300, Thailand
[6] Department of Civil and Construction Engineering, Swinburne University of Technology, Melbourne, VIC 3122, Australia
* Correspondence: suddeepong@g.sut.ac.th

Abstract: Reclaimed asphalt pavement (RAP) contributes substantially to the volume of recycled waste in the world. This research aims to evaluate the mechanistic performance of asphalt concrete with 100% RAP (RAP-AC) modified with natural hemp fiber (HF) reinforcement. The effects of HF lengths and HF contents on the mechanistic performance were investigated. The static tests included Marshall stability, strength index (SI), and indirect tensile strength (ITS), whilst the cyclic tests included indirect tensile resilient modulus (IT M_r), indirect tensile fatigue life (ITFL), and rutting resistance tests. The microstructural analysis revealed that HF could absorb more asphalt cement and function as a reinforcement. The 0.05% HF with a 24 mm HF length was suggested as the best ingredient. For various stress levels, the higher resilience properties—due to the addition of HF—contribute to higher levels of ITFL and rutting resistance. Based on a critical analysis of the cyclic test data, the distress model for HF-RAP-AC was developed for mechanistic pavement design. The outcome of this research promotes the usage of HF-RAP-AC as a greener material for low-traffic roads, which account for over 70% of the total roads worldwide.

Keywords: reclaimed asphalt; natural fiber; asphalt concrete; cyclic performance; waste materials; pavement geotechnics

1. Introduction

Reclaimed asphalt pavement (RAP) contributes substantially to the volume of recycled waste in the world, particularly as more than 95% of the world's roads are flexible pavement. In the past, most RAP is disposed of in landfills. RAP is considered a high-quality recycled material. RAP contents of 30,000 tons with 6% asphalt cement have an equivalent of 28,200 tons of aggregate with 1590 m^3 of asphalt cement. The sustainable innovation for RAP application, therefore, has been developed to maximize RAP usage and mitigate conventional waste disposal. The application of RAP was first developed in 1973 in the United States, and it was only allowed in minimal content for the replacement of natural aggregates (3–5% by total weight of the aggregate) to produce a new pavement [1–9].

El-Maaty and Elmohr (2015) [5]; Shirodkar et al., 2011 [9]; and Zaumanis et al., 2014 [10] revealed that the high amount of aged asphalt cement could lead to inadequate properties in asphalt concretes. The aged asphalt cement causes defective asphalt concrete performance, accelerating premature distress [11,12]. Therefore, many local and international road

authorities have limited the maximum RAP content for flexible pavement construction (5–50% by the weight of the total aggregate).

Conventional natural aggregate production produces 1% of the world's total greenhouse gas emissions due to the mining process; therefore, the application of RAP yields significantly lower environmental effects (35% CO_2eq savings per ton) compared to conventional asphalt concrete [10]. Moreover, RAP is a waste material with a remarkably low aggregate cost compared to natural aggregates. The application of RAP in flexible pavement construction yields a 50–70% savings in total construction cost [10].

However, 100% RAP content reuse is only possible when the RAP has been improved. The mix design modification has been recommended for the application of 100% RAP asphalt concrete. The aged binder content is the prime factor governing the properties of the 100% RAP asphalt concrete mixture. The specific optimum binder content (aged binder + new binder) shall first be determined [10,13]. The mechanistic-related properties require an assessment to evaluate the performance of 100% RAP asphalt concrete. If the properties of 100% RAP asphalt concrete do not meet the requirement, natural aggregate and high-performance asphalt cement need to be used to enhance the mechanical properties [9,11]. Due to the dominant elastic recovery and rheological properties, the polymer-modified asphalt (PMA) with synthetic polymer modifiers, such as the styrene-butadiene-styrene copolymer (SBS), was found to have satisfactory potential for application to the asphalt concrete mixture with high RAP content [14–16]. Synthetic fiber reinforcement is also an effective alternative technology to enhance the performance of asphalt concrete [17,18]. A similar result for synthetic fibers was reported using natural fiber reinforcement [19].

Natural hemp fibers can be considered an effective material for improving the performance of asphalt concretes due to their rough surface (high specific area) with strip protrusions. The hemp network within the asphalt concrete matrix functions as a reinforcing material and can reduce stress concentration-induced failure. Hemp has high durability against environmental damage, resulting in a longer pavement service life. The asphalt concrete with hemp fibers exhibited superior indirect tensile strength, resistance to rutting failure, moisture sensitivity, and cracking failure compared to conventional asphalt concrete [20–22].

Hemp is currently classified as an economic crop in Thailand, which has been supported by Thailand Government for application in the medical, industrial, and education sectors. This research attempts to develop a sustainable 100% RAP-AC strengthened by hemp fibers (HF) for low-traffic roads—which account for more than 70% of Thailand's roads—to support the government's bioeconomy, circular economy, and green economy (BCG model) policies. Thailand's conventional road construction consumes more than 200 million tons/year of natural materials. Therefore, HF-RAP-AC application for Thailand's low-traffic roads could result in a significant reduction in the destruction of ecosystems and the environment.

Theoretically, the wheel load generates the compressive and tensile stresses at the top and bottom of the pavement layers, respectively. Most pavement fatigue distress is caused by tensile traffic stress [23–25]. To evaluate the mechanistic performance of HF-RAP-AC under axle loads, static and dynamic tensile properties tests were performed in this study. The mechanistic performance of HF-RAP-AC, using asphalt cement penetration graded AC60/70 (common asphalt cement in Thailand) at different HF contents and lengths, was determined via indirect tensile resilient modulus, indirect tensile fatigue, and rutting resistance tests. A microstructure analysis was performed to examine the influence of the HF content and length on the mechanistic performance of the RAP-AC samples. The results of tensile strain and fatigue life were analyzed to develop the distress model for various HF contents and lengths. The outcome of this research will promote the application of HF-RAP-AC in road infrastructure as a green construction material.

2. Materials

2.1. Hemp Fiber (HF)

The studied HF was obtained from local handicrafts from a community enterprise group in the Chiang Mai province north of Thailand. The raw HF was subjected to a quality treatment process to prevent deterioration due to environmental damage. The raw HF was sun-dried for approximately 7 days and thereafter boiled at 100 degrees Celsius. During the boiling process, additives, such as carbon agents, fungicides, moisture repellents, and UV protection agents, were mixed with the HF for 1 h. The treated HF was next air-dried for approximately 7 days and woven into the thread. The studied HF is presented in Figure 1. The basic properties of the studied HF are summarized in Table 1.

Figure 1. Studied HF.

Table 1. Basic and engineering properties of HF.

Properties	Unit	Test Method	Results
Tensile strength	N	TIS-121	10.21
Tenacity	(gf/Tex)	TIS-121	47.03
Elongation	%	TIS-121	5.85
Size	Tex	TIS-121	181.6
Moisture content	%	ASTM D 629	6.76

Remark: 1 Tex = 1 g/1000 m.

2.2. Asphalt Cement (AC)

The ordinary asphalt cement for Thailand's flexible pavement construction, asphalt cement penetration grade 60/70, was selected for this study. According to the standard for asphalt cement selection specified by the Department of Highways, Thailand [26], the properties of AC60/70 met the minimum requirement, as summarized in Table 2.

Table 2. Basic and engineering properties of asphalt cement AC60/70.

| Properties	Units	Test Method	Specifications	Results
Penetration	-	DH-T 403	60–70	67
Flash point	°C	DH-T 406	>232	332
Ductility 25 °C	cm	DH-T 405	>100	150
Solubility in trichloroethylene	%wt	DH-T 409	>99.0	99.97
Test on residue from thin film oven test (5 h @ 163 °C)				
Weight loss	%	DH-T 404	<0.8	0.12
Penetration	% of original.	DH-T 403	>54	71.1
Ductility 25 °C	cm	DH-T 405	>50	150

2.3. RAP Aggregate

The RAP aggregate was supplied by the Office of Nakhon Ratchasima Highways, Thailand. The aged asphalt cement content of the RAP aggregate was determined using method A in accordance with ASTM D2172 [27]. Thereafter, the basic and engineering properties of the RAP aggregate were determined based on the standard for asphalt hot mix recycling specified by the Thailand Department of Highways [28]. The RAP properties are summarized in Table 3.

**Table 3.** Basic and engineering properties of the RAP aggregate.

Properties	Unit	Test Method	Specifications	Results
Soundness	%	DH-T 213	<9	10.21
Los Angeles abrasion, LA	%	DH-T 202	<40	47.03
Flakiness index	%	DH-T 210	<35	33.00
Elongation index	%	DH-T 211	<35	34.00
Asphalt content in RAP	%	ASTM D 2172	-	5.67

2.4. Mix Design and Sample Preparation

The RAP-AC mixture was designed as recommended by Zaumanis et al., (2014) [10]. The RAP aggregate was sieved, and its gradation was adjusted to meet the specification for the pavement surface wearing course in accordance with DH-S 410/1999 [28] (Figure 2). Using the Marshall method, the optimum asphalt cement at 4% air void of the RAP-AC mixture was determined. The total asphalt cement content (aged asphalt cement + added asphalt cement) was allowed in the range between 6 and 9% of the total weight of the mixture. To meet the 4% air void, 7% total asphalt cement content (5.67% aged asphalt content + 1.33% added asphalt content) was selected, as presented in Figure 3.
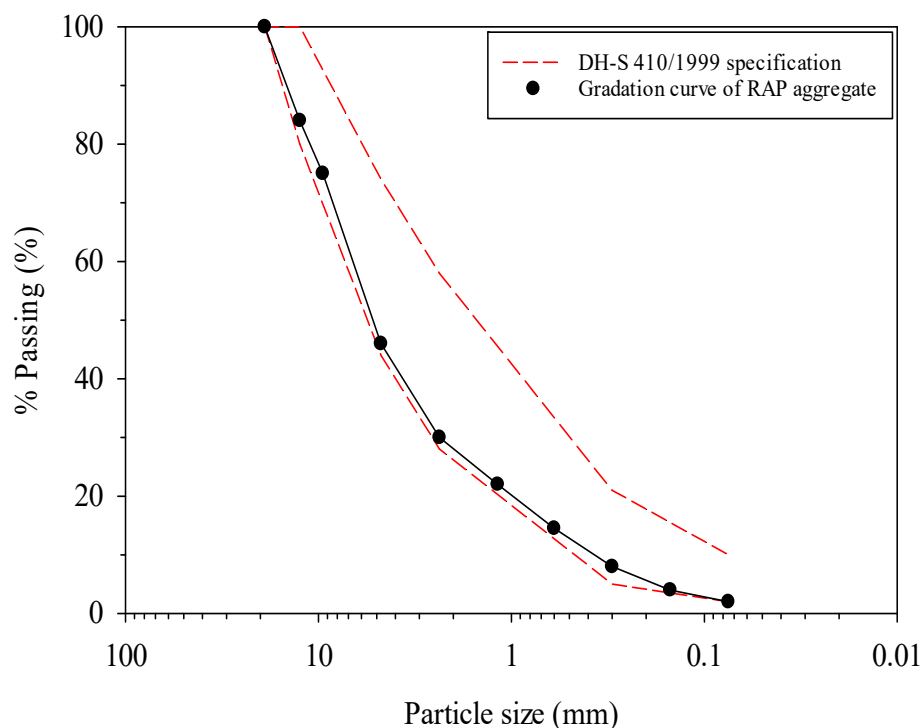
Figure 2. Particle size distribution of the RAP aggregate.
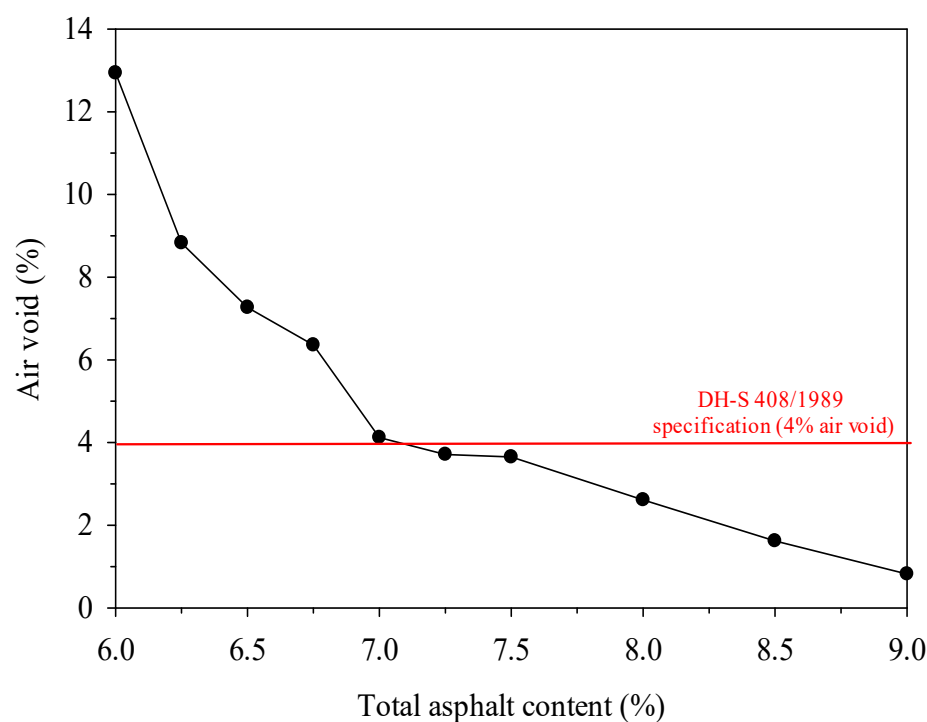
Figure 3. Relationship between the air void and total asphalt cement content of RAP-AC samples.

In order to assess the effect of fiber reinforcement on the performance of RAP-AC, HF with lengths of 20, 22, and 24 mm, typically used for synthetic fiber-modified asphalt concretes [18], was added as an additive at various contents of 0, 0.05, 0.1, and 0.25% by dry weight of the total aggregate. The HF-modified RAP-AC samples were prepared in accordance with DH-S 410/1999 [28] at 4% air void using the Marshall method. The AC60/70 and RAP aggregate were heated at 170 °C and 160 °C, respectively [28]. The HF-RAP-AC mixture was then mixed within 60 s at 150 °C, and compacted for 75 blows on each side in a metallic mold (101.60 mm in diameter). The static and cyclic tests were then conducted on the mixtures with the target HF contents and lengths.

3. Experimental Program

3.1. Marshall Stability

The Marshall stability of the HF-RAP-AC samples was assessed according to ASTM D6927 [29]. The HF-RAP-AC was installed in the standard load frame before being sub-jected to vertical loading at a 50 mm/min deformation rate using a compression machine with automatic load and deformation recorders.

3.2. Strength Index (SI)

The strength index (SI) was performed to assess the potential of HF-RAP-AC to resist binder peeling due to the corrosion of sodium chloride, according to DH-S 413/2001 [30]. The HF-RAP-AC sample was soaked in sodium chloride (5 g per 0.001 m^3) at 60 °C using an automatically controlled temperature water bath for 24 h; then, it was removed and soaked in water at 25 °C for 1 h. The SI value is the Marshall stability ratio of the soaked to the unsoaked RAP-AC samples.

3.3. Indirect Tensile Strength (ITS)

The tensile strength of HF-RAP-AC was evaluated via the indirect tensile method in accordance with ASTM D6931 [31]. The HF-RAP-AC sample was installed at the indirect tensile loading frame inside a controlled temperature chamber. Prior to the test, the target temperatures of 25, 40, and 50 °C were controlled to evaluate the resistance to strength

degradation at the raised temperatures. The sample was then subjected to vertical stress at the deformation rate of 50 mm/min at the target temperature.

3.4. Indirect Tensile Resilient Modulus (IT M_r)

The resilient properties of HF-RAP-AC under repetitive stress were determined via an indirect tensile resilient modulus test according to ASTM D4123 [32]. The HF-RAP-AC sample was installed within the standard loading equipment. Thereafter, the sample was subjected to a haversine loading pulse with a loading frequency of 1.0 Hz (0.1 s loading period and 0.9 s rest period) at a stress level of 15% ITS, based on the ASTM D4123 [32] recommendation. The repetitive stress was applied to the sample for 200 cycles. In each cycle, the horizontal deformation was measured using LVDT connected with an automatic data recorder.

3.5. Indirect Tensile Fatigue (ITF)

The resistance of the HF-RAP-AC samples to fatigue failure was examined using an indirect tensile fatigue test based on EN 12697-24 [33]. The haversine load pulse with the same frequency as that for the IT M_r test was applied at the stress levels of 250, 300, and 350 kPa. The repetitive stress was continuously applied until the sample failed.

3.6. Rutting Resistance

The resistance of the HF-RAP-AC samples to rutting failure was determined based on AASHTO T324 [34] via the Hamburg wheel tracker testing machine. The HF-RAP-AC sample, with a diameter of 150 mm and thickness of 60 mm, was subjected to the repetitive wheel load at a stress level of 1.5 kN for 10,000 cycles. The rutting failure resistance was described in terms of the rut depth.

3.7. Microstructural Analysis

The microstructural analysis was carried out using scanning electron microscopy (SEM) to analyze the effect of HF content and length on the mechanical properties. The 100 and 150× magnifications were selected for this purpose. The SEM sample was collected from the fraction of the mechanical testing sample. The sample was freeze-dried using liquid nitrogen at the temperature of −195 °C and then gold coated.

4. Results

4.1. Experimental Results

At 7% total asphalt cement content, the higher HF content resulted in a higher air void (more than 4%) for all HF lengths, as presented in Figure 4. Even with the same HF content, the HF with a higher length has a higher air void for the same asphalt content. To keep the 4% air void constant, a higher binder content is required. The optimum binder contents of HF-RAP-AC are summarized in Figure 5. The increased optimum binder content of HF-RAP-AC with higher HF content is attributed to the higher pores of HF [35].

The Marshall stability of HF-RAP-AC at different HF lengths and contents is illustrated in Figure 6. The solid line shows the minimum stability requirement of 8 kN specified by DH-S 408/1989 [36]. Both RAP-AC and HF-RAP-AC samples met the requirement to be used as the surface-wearing course. The addition of HF contributed to the Marshall stability improvement for RAP-AC samples. The improved stability might be attributed to the higher optimum binder content (Figure 5). For example, the Marshall stability of HF-RAP-AC samples with 0.05% HF content at 20, 22, and 24 mm HF lengths was 10.47, 10.98, 11.09, and 11.30 kN, corresponding to the AC60/70 contents of 7.07, 8.05, 8.22, and 8.50%, respectively. The higher HF content resulted in a higher stability value at the same HF length, and vice versa. The highest stability value was found at the highest HF content and the longest HF tested (0.25% HF content and 24 mm HF length) of 12.15 kN.
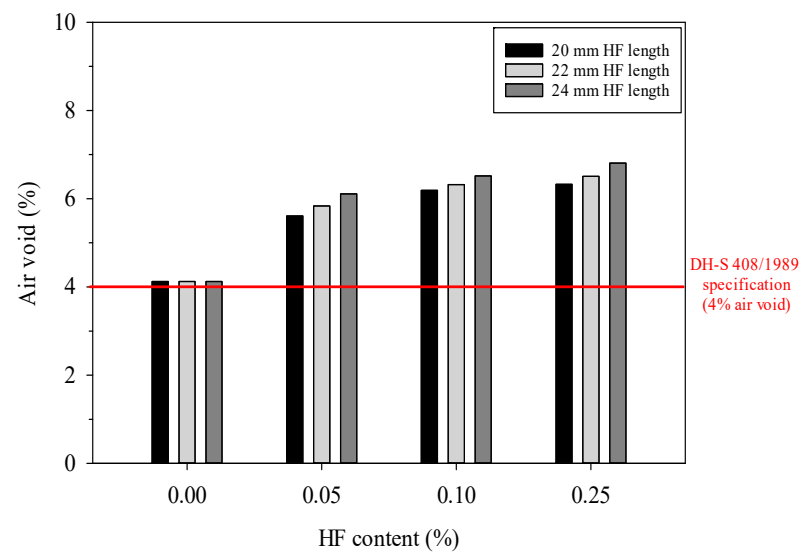
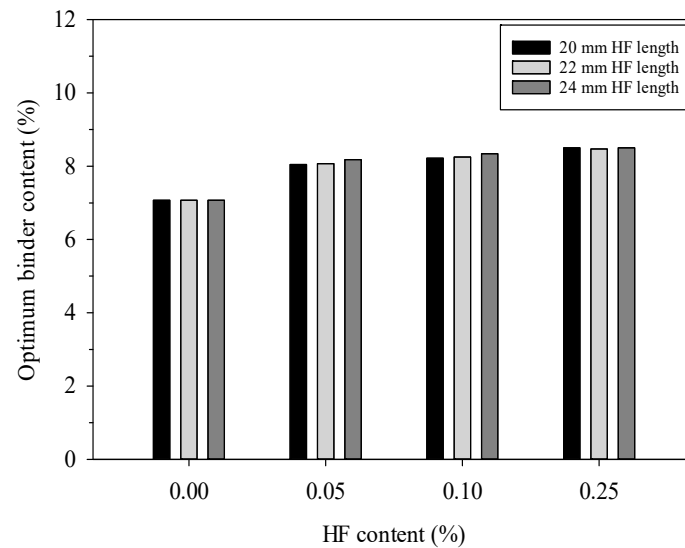**Figure 4.** Relationship between the air void and HF content of the HF-RAP-AC samples.

Figure 5. Optimum binder content of the HF-RAP-AC samples at different HF contents.
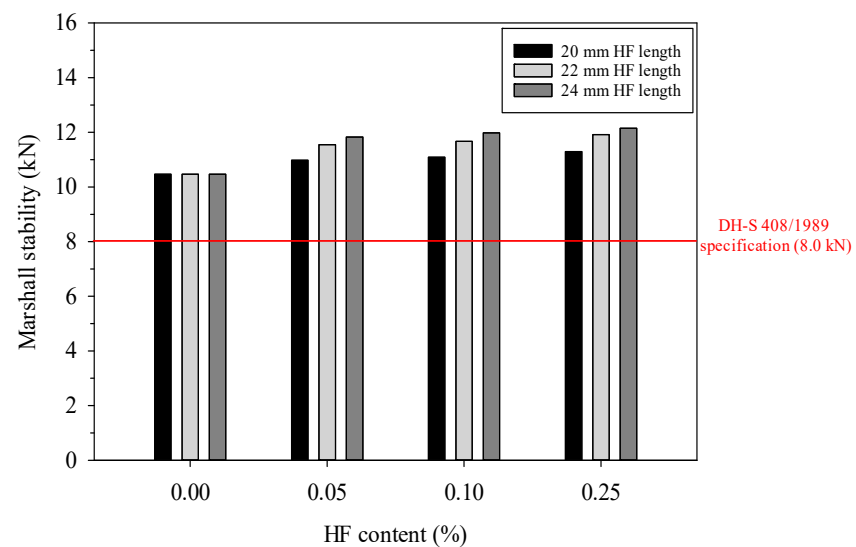

Figure 6. Relationship between Marshall stability and HF content of HF-RAP-AC samples.

To examine the role of HF in stability improvement, the HF-stability/0%HF-stability (the stability ratio of HF-RAP-AC sample to RAP-AC sample) was investigated, as illustrated in Figure 7. Both HF length and content affected stability improvement. The 0.05% HF was the most effective HF content for all HF lengths, whereby the HF-stability/0%HF-stability was equal to 1.05, 1.10, and 1.13 for the lengths of 20, 22, and 24 mm, respectively. Although higher HF content (more than 0.05%) contributed to a higher HF-stability/0%HF-stability ratio value, the development rate was relatively small. For example, at 20 mm HF length, the HF-stability/0%HF-stability values were 1.05, 1.06, and 1.08 for 0.05, 0.10, and 0.25% HF contents, respectively. This 0.05% content is also recommended for synthetic fibers modified asphalt concretes [35].
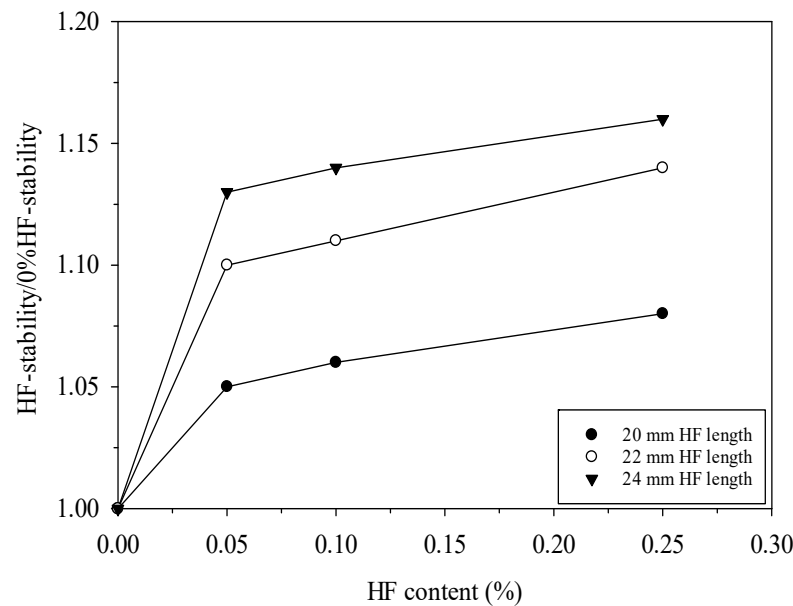
Figure 7. Relationship between HF-stability/0%HF-stability and HF content of the HF-RAP-AC samples.

The SI values of the HF-RAP-AC samples at different HF lengths and contents are presented in Figure 8. The solid line represents the minimum requirement of the 80% SI value according to DH-S 408/1989 [36]. Without HF, the SI value of the RAP-AC sample did not meet the minimum requirement (lower than 80%), showing the negative effect of aged asphalt cement. The additional HF contributed to SI improvement, whereby the SI met the minimum requirement when >0.05% HF was introduced for all HF lengths. In other words, high binder content due to the HF inclusion enhanced the adhesion strength and, at the same time, strengthened the resistance to binder peeling. Similar to the stability result, both HF length and content directly affected SI improvement; the highest SI value of 92% was found at the highest HF content of 0.25% and the longest length of 24 mm. The 0.05% HF was the threshold limit separating active and inert improvement. The SI value of 0.25% HF-RAP-AC was only approximately 5.5% higher than the 0.05% HF-RAP-AC for all HF lengths. The 0.05% HF-RAP-AC with a 22 mm HF length had an 11.4% lower SI value than the 0.05% HF-RAP-AC with a 24 mm HF length, thus indicating the significant effect of HF length.

The ITS values of the HF-RAP-AC at different HF lengths and contents under different temperatures are presented in Figure 9. The high temperature weakened the binder adhesion strength, hence reducing the ITS value for all samples. The addition of HF could effectively enhance the ITS of RAP-AC, even at very high temperatures. For all temperatures tested, the highest ITS was found at 0.25% HF-RAP-AC with a 24 mm HF length. Figure 9 shows that the HF length had a more pronounced effect on the ITS improvement than the HF content. At the same temperature and HF length of 20 mm, the ITS improvement for 0.05% HF was 19.6% benchmarked with 0% HF, whereas the ITS improvement for 0.25% HF was only 26.2% benchmarked with 0% HF. However, the 0.05% HF-RAP-AC with a

24 mm HF length had 20.6% higher ITS improvement than the 0.05% HF-RAP-AC with a 20 mm HF length.
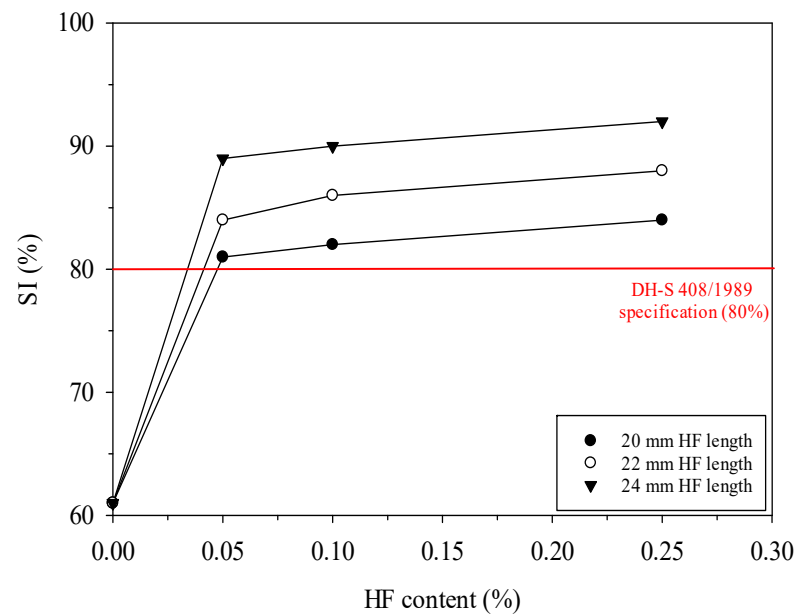

Figure 8. Relationship between SI and HF content of the HF-RAP-AC samples.
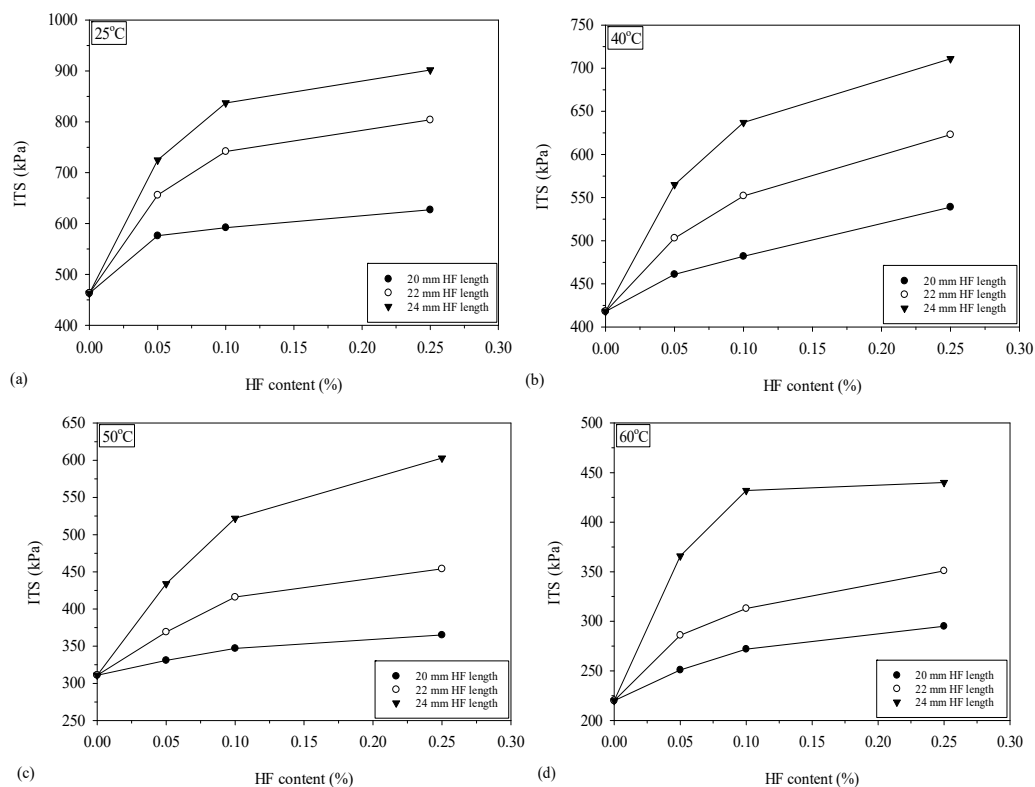

Figure 9. Relationship between ITS and HF content of the HF-RAP-AC samples at (**a**) 25 °C, (**b**) 40 °C, (**c**) 50 °C, and (**d**) 60 °C.

The relationship between IT M_r versus HF content at different HF lengths of the HF-RAP-AC samples is demonstrated in Figure 10. Similar to the ITS result, the addition of HF significantly enhanced the resilient properties of HF-RAP-AC for all HF lengths and contents up to the highest value at 0.25% HF-RAP-AC with a 24 mm HF length. The 0.05% HF was the best HF content; the 0.05% HF-RAP-AC samples had higher IT M_r values than

the 0% HF-RAP-AC sample, which were 11.1, 14.9, and 20.2% for the 20, 22, and 24 mm HF lengths, respectively.
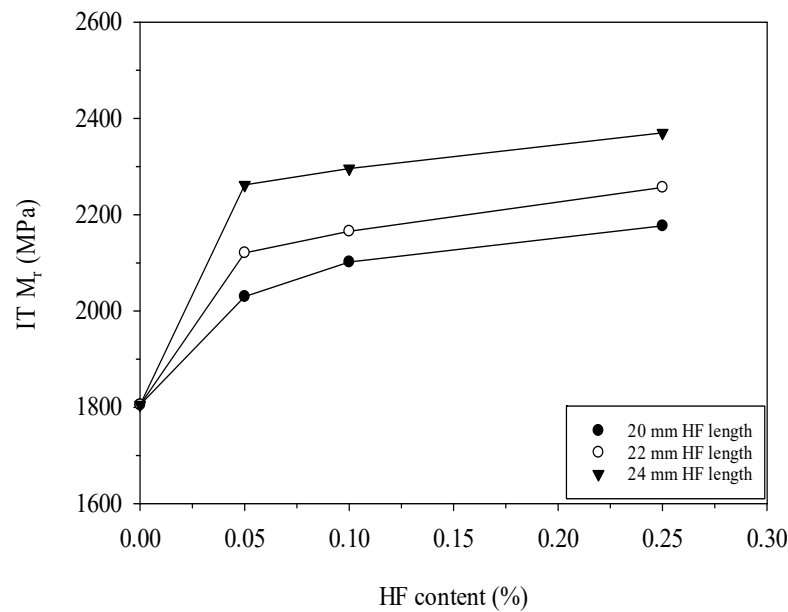

Figure 10. Relationship between IT Mr and HF content of the HF-RAP-AC samples.

Theoretically, the asphalt concretes with superior ITS exhibit excellent resistance to recoverable deformation, hence the high IT M_r [37]. As such, it is logical to develop a relationship between IT M_r and ITS for HF-RAP-AC and RAP-AC, as illustrated in Figure 11, with a high degree of correlation of 0.90.

$$IT\ M_r = 1275 + 1261ITS \tag{1}$$
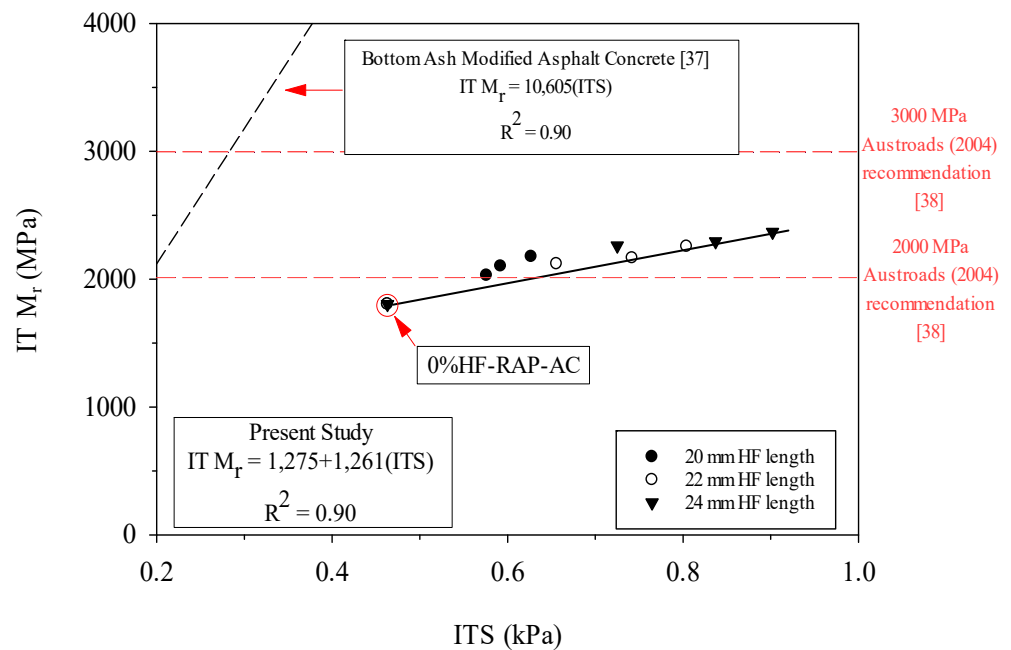
Figure 11. Relationship between IT Mr and ITS of the HF-RAP-AC samples.

When compared with available data for AC60/70 and 4% air void [37], it was evident that even with the HF addition, the normal AC and bottom ash-modified AC had higher IT M_r values than the RAP-AC at the same ITS. Even though the HF-RAP-AC had compa-

rable Marshall stability values to the normal AC, the IT M_r was significantly lower and, therefore, suitable for the low-traffic road. Based on Austroads (2004) [38], the IT M_r values of HF-RAP-AC met the requirement for the surface-wearing course of low-traffic roads (2200–3000 MPa) [39].

The relationships between indirect tensile fatigue life (ITFL) versus stress level at various HF contents and HF lengths are illustrated in Figure 12. The higher stress level caused considerably more plastic deformation, consequently leading to a significantly lower ITFL for all samples. At the same stress level, due to the improved resilient properties, the addition of HF contributed to the higher ITFL. The 0.25% HF-RAP-AC with a 24 mm HF length exhibited the highest ITFL value for all stress levels. It was found that the HF-RAP-AC had a higher ITFL at the same stress level than the bottom ash-modified AC for the same limestone aggregate and 4% air void [37].
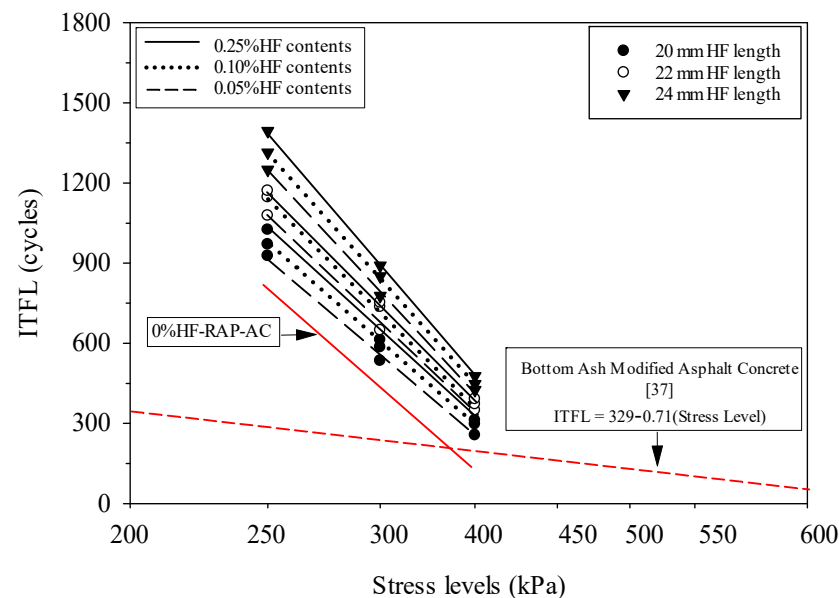

Figure 12. Relationship between ITFL and stress levels at different HF content and HF length of the HF-RAP-AC samples.

The increased stress level (from 250 to 350 kPa) caused a reduction in the ITFL of the 0% HF-RAP-AC sample by 80%. The HF addition can prevent the reduction in ITFL; for an HF length of 22 mm, the ITFL of 0.05% HF-RAP-AC decreased with the increased stress level by 72%, and the ITFL of 0.25% HF-RAP-AC decreased by 70%. Meanwhile, the ITFL of 0.05% HF-RAP-AC with a 24 mm length decreased with the increased stress level by only 66%. In other words, the increased HF content (0.05% HF to 0.25% HF) at a 22 mm length resulted in a 2% improvement in ITFL. However, for HF content of 0.05%, the increased HF length (22 mm to 24 mm) resulted in a 6% improvement in ITFL.

Figure 13 illustrates the relationship between the rut depth at 10,000 cycles of the wheel load versus the HF content of the HF-RAP-AC for various HF lengths. The RAP-AC sample (without HF) failed before achieving the target of 10,000 cycles, as presented in Figure 14a. The addition of HF improved the rutting resistance of the RAP-AC sample, as shown in Figure 14b–d. The smallest rut depth was clearly detected for the longest HF, as shown in Figure 14d; the 0.25% HF-RAP-AC with a 24 mm HF length exhibited the lowest rut depth of 2.91 mm.

The longer HF length played a more important role in the rutting resistance than the higher HF content. For example, the rut depths of 0.05% HF-RAP-AC with 20, 22, and 24 mm HF lengths were 11.92, 7.45, and 3.54 mm, respectively, whereas the values were 11.92, 10.30, and 8.06 mm for HF-RAP-AC with 20 mm at 0.05, 0.10, and 0.25% HF contents, respectively.
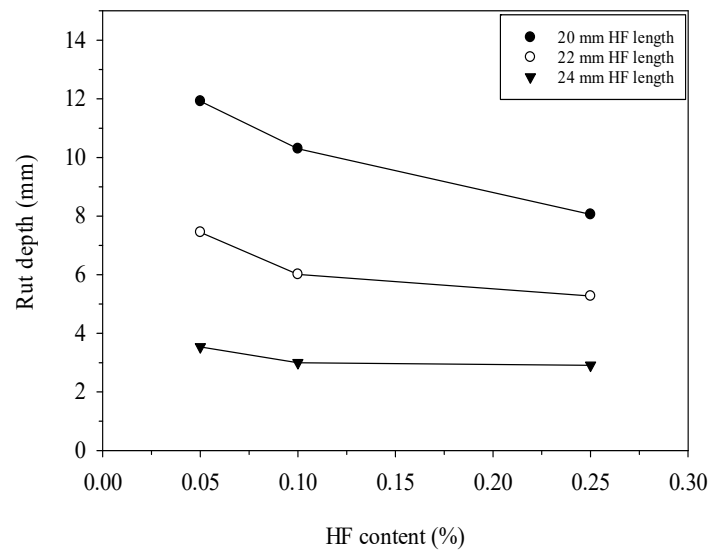
Figure 13. Relationship between rut depth and HF content of the HF-RAP-AC samples.
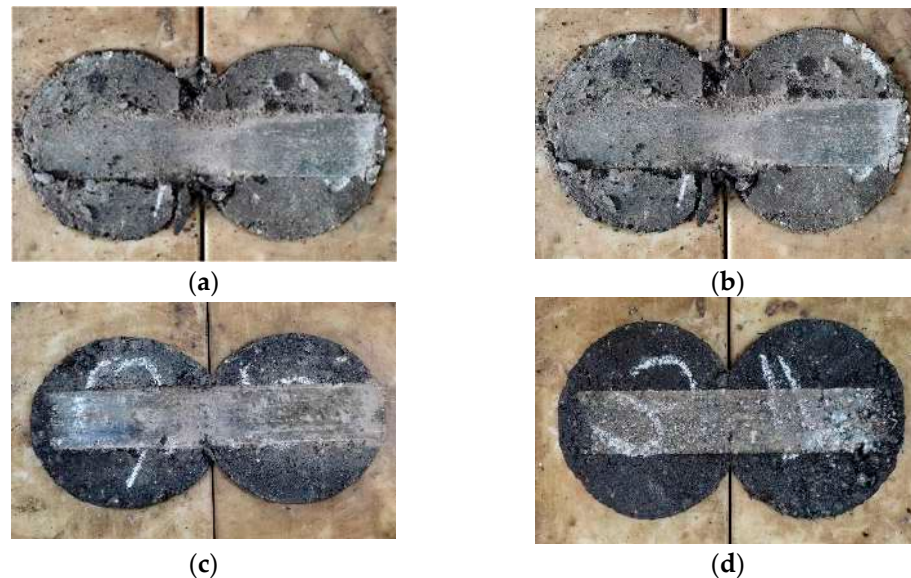
Figure 14. Failure characteristics of (**a**) 0% HF-RAP-AC and 0.05% HF-RAP-AC samples with (**b**) 20, (**c**) 22, and (**d**) 24 mm HF lengths.

Since asphalt concrete is more or less a homogeneous and isotropic material, the improved tensile resilient properties resulted in improved compression-resilient properties. As such, the influence of IT M_r on the rutting resistance of the HF-RAP-AC was investigated and is demonstrated in Figure 15. The higher IT M_r was associated with a lower rut depth at the same target wheel cycles. In other words, the HF not only functioned as a tensile reinforcement but also, at the same time, effectively improved bearing resistance.

The microstructural image of HF-RAP-AC is presented in Figure 16. The HF had the ability to absorb asphalt cement (Figure 16a), hence improving the adhesion strength between the aggregate and binder. As such, the higher HF content and length resulted in HF-RAP-AC performance improvement due to the higher optimum asphalt cement. In addition to adhesion strength improvement, the HF functioned as a reinforcement within the microstructure observed by the twist fibers (Figure 16b). A similar result of the natural fiber as a reinforcement in the polymer material has also been reported [40]. Therefore, the HF with a longer length had a superior ability to provide an interlocking to the aggregate structure, resulting in a more dominant effect on performance improvement.
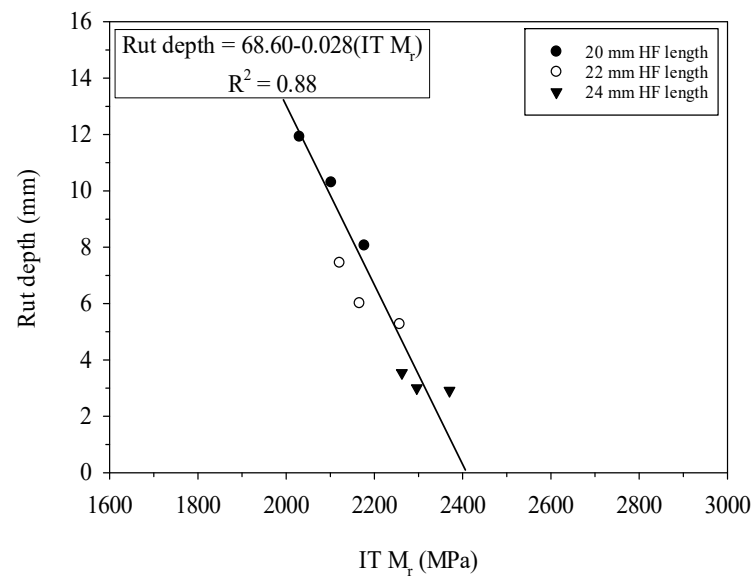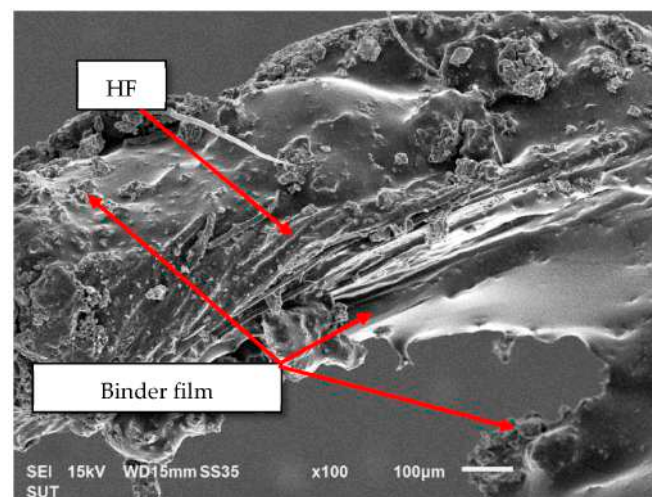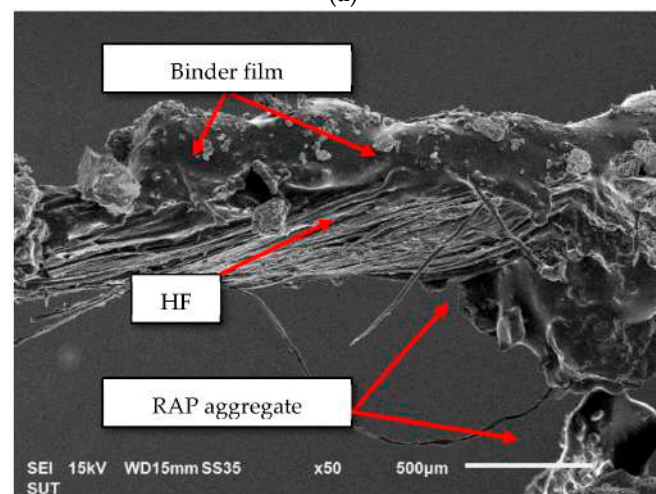
Figure 15. Relationship between rut depth and IT Mr of the HF-RAP-AC samples.

(**a**)

(**b**)

Figure 16. Microstructure image of HF-RAP-AC samples at (**a**) HF coated by binder within the HF-RAP-AC matrix at $100\times$ magnifications, (**b**) HF coated by binder within the HF-RAP-AC matrix at $50\times$ magnifications.

4.2. Distress Model of HF-RAP-AC

Based on EN 12697-24 [33], the tensile fatigue life (N_f) is directly related to the initial tensile strain (ε_t) in the logarithm relationship. The general fatigue distress model is, therefore, developed in terms of the initial tensile strain:

$$N_f = a\left[\frac{1}{\varepsilon_t}\right]^b \tag{2}$$

where a and b are the fatigue parameters, which depend upon the material characteristic.

$$\varepsilon_t = \frac{\sigma(1+3v)}{\text{IT M}_r} \tag{3}$$

where σ is the applied stress level (kPa) and v is Poisson's ratio (assumed to be 0.35, based on EN 12697-24 [33]).

The different pavement materials exhibit different tensile strains at the same number of cycles due to the difference in material properties and, consequently, the difference in fatigue life. As such, the destress model for HP-RAP-AC is required for pavement surface design at various traffic volumes. The distress model of HF-RAP-AC was developed based on the analysis of the cyclic test data (Figure 17) as follows:

$$N_f = 3.4 \times 10^{11}\left[\frac{1}{\varepsilon_t}\right]^{3.562} \tag{4}$$
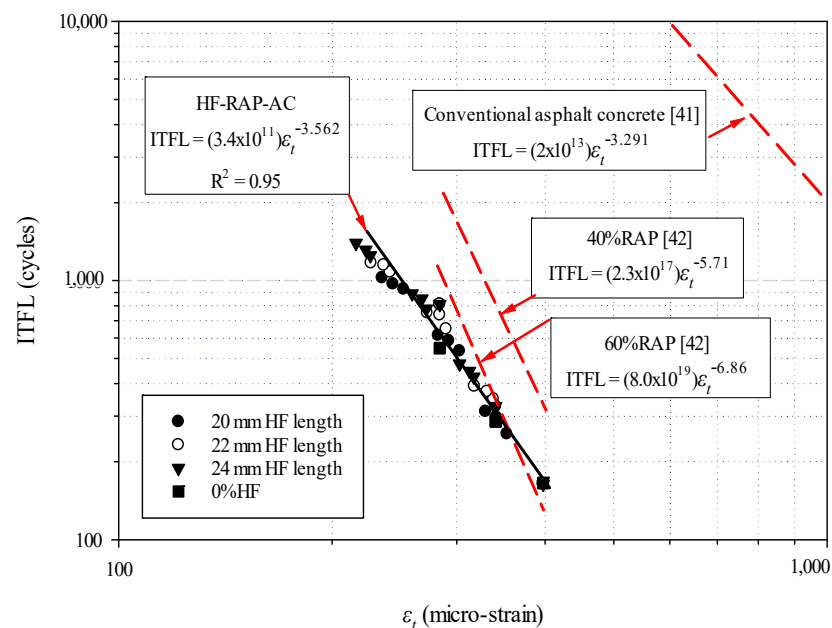
Figure 17. Relationship between ITFL and ε_t of HF-RAP-AC with and without HF samples.

The proposed distress model of HF-RAP-AC was a logarithm relationship, irrespective of HF content and length. Even though the destress model was the same, the fatigue life was different because the IT M_r, which governs the tensile strain, was different depending on the HF content and length. The HF-RAP-AC with higher IT M_r exhibited a lower tensile strain and higher fatigue life for the same traffic loads. The IT M_r of the HF-RAP-AC could practically be approximated from Equation (1) using the ITS, which was simply obtained using a conventional laboratory test. It was evident that the proposed model had a similar function to the distress model of conventional asphalt concrete by AI (1983) [41]. The b values were found to be more or less the same, while the a value of the proposed model was lower due to the negative effect of aged asphalt cement.

5. Conclusions

This research evaluated the mechanistic performance of hemp fiber-modified asphalt concrete with reclaimed asphalt pavement, HF-RAP-AC, for low-traffic roads. The following significant findings can be summarized from this research:

1. The HF-RAP-AC required higher optimum binder content due to the high asphalt cement absorbability of porous HF. The higher HF content and length possessed a higher optimum binder content. The microstructural analysis, moreover, revealed the function of HF as a reinforcement within the microstructure.

2. The best mechanistic performance of HF-RAP-AC was found for the 0.25% HF-RAP-AC with a 24 mm HF length. HF length had a more pronounced effect on the mechanistic performance improvement than the HF content. The 0.05% HF was suggested as the most effective HF content for all HF lengths. Beyond this HF content (>0.05%), the rate of mechanistic property improvement was relatively low.

3. Even though the HF-RAP-AC had comparable Marshall stability levels to the normal AC, the IT M_r was significantly lower. Therefore, the HF-RAP-AC is suitable for low-traffic applications, whereby its IT M_r values meet the requirement for the surface-wearing course of low-volume roads suggested by Ausroads (2004).

4. The higher ITS contributed to a higher IT M_r in the linear relationship, irrespective of HF content and length. At the same stress level, the improved resilient properties due to the addition of HF contributed to the improved ITFL and rutting resistance of the HF-RAP-AC.

5. The distress model of HF-RAP-AC was found to be unique for various HF contents and lengths. Even though the destress model was the same, the fatigue life was different because the IT M_r, which governs the tensile strain, was different depending on the HF content and length. The HF-RAP-AC with higher IT M_r exhibited a lower tensile strain and higher fatigue life for the same traffic loads. This proposed distress model is useful for mechanistic pavement design methods for low-traffic roads, which support the sustainable construction policy in Thailand and other countries worldwide.

References

1. Debbarma, S.; Selvam, M.; Singh, S. Can flexible pavements' waste (RAP) be utilized in cement concrete pavements—A critical review. *Constr. Build. Mater.* **2020**, *259*, 120417. [CrossRef]
2. Yaghoubi, E.; Ahadi, M.R.; Alijanpour Sheshpoli, M.; Jahanian Pahlevanloo, H. Evaluating the performance of hot mix asphalt with reclaimed asphalt pavement and heavy vacuum slops as rejuvenator. *Int. J. Transp. Eng.* **2013**, *1*, 115–124.
3. Yaghoubi, E.; Sudarsanan, N.; Arulrajah, A. Stress-strain response analysis of demolition wastes as aggregate base course of pavements. *Transp. Geotech.* **2021**, *30*, 100599. [CrossRef]
4. Yaghoubi, E.; Disfani, M.M.; Arulrajah, A.; Kodikara, J. Development of a void ratio-moisture ratio-net stress framework for the prediction of the volumetric behavior of unsaturated granular materials. *Soils Found.* **2019**, *59*, 443–457. [CrossRef]
5. El-Maaty, A.E.A.; Elmohr, A.I. Characterization of recycled asphalt pavement (RAP) for use in flexible pavement. *Am. J. Eng. Appl. Sci.* **2015**, *8*, 233–248. [CrossRef]
6. Gautam, P.K.; Kalla, P.; Jethoo, A.S.; Agrawal, R.; Singh, H. Sustainable use of waste in flexible pavement: A review. *Constr. Build. Mater.* **2018**, *180*, 239–253. [CrossRef]
7. Monu, K.; Ransinchung, G.; Singh, S. Effect of long-term ageing on properties of RAP inclusive WMA mixes. *Constr. Build. Mater.* **2019**, *206*, 483–493. [CrossRef]
8. Reyes-Ortiz, O.; Berardinelli, E.; Alvarez, A.E.; Carvajal-Muñoz, J.; Fuentes, L. Evaluation of hot mix asphalt mixtures with replacement of aggregates by reclaimed asphalt pavement (RAP) material. *Procedia-Soc. Behav. Sci.* **2012**, *53*, 379–388. [CrossRef]
9. Shirodkar, P.; Mehta, Y.; Nolan, A.; Sonpal, K.; Norton, A.; Tomlinson, C.; Dubois, E.; Sullivan, P.; Sauber, R. A study to determine the degree of partial blending of reclaimed asphalt pavement (RAP) binder for high RAP hot mix asphalt. *Constr. Build. Mater.* **2011**, *25*, 150–155. [CrossRef]
10. Zaumanis, M.; Mallick, R.B.; Frank, R. 100% recycled hot mix asphalt: A review and analysis. *Resour. Conserv. Recycl.* **2014**, *92*, 230–245. [CrossRef]
11. Celauro, C.; Bernardo, C.; Gabriele, B. Production of innovative, recycled and high-performance asphalt for road pavements. *Resour. Conserv. Recycl.* **2010**, *54*, 337–347. [CrossRef]
12. George, A.M.; Banerjee, A.; Puppala, A.J.; Saladhi, M. Performance evaluation of geocell-reinforced reclaimed asphalt pavement (RAP) bases in flexible pavements. *Int. J. Pavement Eng.* **2021**, *22*, 181–191. [CrossRef]
13. Elkashef, M.; Williams, R.C. Improving fatigue and low temperature performance of 100% RAP mixtures using a soybean-derived rejuvenator. *Constr. Build. Mater.* **2017**, *151*, 345–352. [CrossRef]
14. Mogawer, W.S.; Austerman, A.J.; Kluttz, R.; Roussel, M. High-performance thin-lift overlays with high reclaimed asphalt pavement content and warm-mix asphalt technology: Performance and workability characteristics. *Transp. Res. Rec.* **2012**, *2293*, 18–28. [CrossRef]
15. Yan, Y.; Roque, R.; Cocconcelli, C.; Bekoe, M.; Lopp, G. Evaluation of cracking performance for polymer-modified asphalt mixtures with high RAP content. *Road Mater. Pavement Des.* **2017**, *18* (Suppl. S1), 450–470. [CrossRef]
16. Yan, Y.; Roque, R.; Hernando, D.; Chun, S. Cracking performance characterisation of asphalt mixtures containing reclaimed asphalt pavement with hybrid binder. *Road Mater. Pavement Des.* **2019**, *20*, 347–366. [CrossRef]
17. Jaskuła, P.; Stienss, M.; Szydłowski, C. Effect of polymer fibres reinforcement on selected properties of asphalt mixtures. *Procedia Eng.* **2017**, *172*, 441–448. [CrossRef]
18. Takaikaew, T.; Hoy, M.; Horpibulsuk, S.; Arulrajah, A.; Mohammadinia, A.; Horpibulsuk, J. Performance improvement of asphalt concretes using fiber reinforcement. *Heliyon* **2021**, *7*, e07015. [CrossRef]
19. Abiola, O.; Kupolati, W.; Sadiku, E.; Ndambuki, J. Utilisation of natural fibre as modifier in bituminous mixes: A review. *Constr. Build. Mater.* **2014**, *54*, 305–312. [CrossRef]
20. Gallo, P. Asphalt mix reinforced with vegetable fibers. In *IOP Conference Series: Materials Science and Engineering*; IOP Publishing: Bristol, UK, 2017.
21. Gallo, P.; Valentin, J. Stone mastic asphalt reinforced by vegetable yarns. In *International Conference on Sustainable Materials, Systems and Structures (SMSS2019): New Generation of Construction Materials*; RILEM Publications: Reykjavik, Iceland, 2019.
22. Shanbara, H.K.; Ruddock, F.; Atherton, W. A laboratory study of high-performance cold mix asphalt mixtures reinforced with natural and synthetic fibres. *Constr. Build. Mater.* **2018**, *172*, 166–175. [CrossRef]
23. Gupta, S.; Veeraragavan, A. Fatigue behaviour of polymer modified bituminous concrete mixtures. *Pap. Presented J. Indian Road Congr.* **2009**, *70*, 548.
24. Mashaan, N.S.; Ali, A.H.; Koting, S.; Karim, M.R. Dynamic properties and fatigue life of stone mastic asphalt mixtures reinforced with waste tyre rubber. *Adv. Mater. Sci. Eng.* **2013**, *2013*, 319259. [CrossRef]
25. Modarres, A.; Hamedi, H. Developing laboratory fatigue and resilient modulus models for modified asphalt mixes with waste plastic bottles (PET). *Constr. Build. Mater.* **2014**, *68*, 259–267. [CrossRef]
26. *DH-SP 401/1988*; Specification for Asphalt Cement. Department of Highway: Bangkok, Thailand, 1988.
27. *ASTM D2172-05*; Standard Test Methods for Quantitative Extraction of Bitumen from Bituminous Paving Mixtures. American Society for Testing and Materials (ASTM): West Conshohocken, PA, USA, 2004.
28. *DH-S 410/1999*; Asphalt Hot-Mix Recycling. Department of Highway: Bangkok, Thailand, 1999.
29. *ASTM D6927-15*; Standard Test Method for Marshall Stability and Flow of Asphalt Mixtures. American Society for Testing and Materials (ASTM): West Conshohocken, PA, USA, 2015.

30. *DH-S 413/2001*; Strength Index. Department of Highway: Bangkok, Thailand, 2001.
31. *ASTM D6931-12*; Standard Test Method for Indirect Tensile (IDT) Strength of Bituminous Mixtures. American Society for Testing and Materials (ASTM): West Conshohocken, PA, USA, 2012.
32. *ASTM D4123-82*; Standard Test Method for Indirect Tension Test for Resilient Modulus of Bituminous Mixtures. American Society for Testing and Materials (ASTM): West Conshohocken, PA, USA, 1995.
33. *EN 12697-24*; Bituminous Mixtures—Tests Methods for Hot Mix Asphalt—Part 24: Resistance to Fatigue, European Standard. CEN (European Committee for Standardization): Brussels, Belgium, 2007.
34. *AASHTO T 324*; Hamburg Wheel-Track Testing of Compacted Hot Mix Asphalt (HMA). AASHTO: Washington, DC, USA, 2014.
35. Phan, T.M.; Nguyen, S.N.; Seo, C.B.; Park, D.W. Effect of treated fibers on performance of asphalt mixture. *Constr. Build. Mater.* **2021**, *274*, 122051. [CrossRef]
36. *DH-S 408/1989*; Asphalt Concrete or Hot-Mix Asphalt. Department of Highway: Bangkok, Thailand, 1989.
37. Buritatum, A.; Suddeepong, A.; Horpibulsuk, S.; Akkharawongwhatthana, K.; Yaowarat, T.; Hoy, M.; Arulrajah, A. Improved Performance of Asphalt Concretes using Bottom Ash as an Alternative Aggregate. *Sustainability* **2022**, *14*, 7033. [CrossRef]
38. Design, P. *A Guide to the Structural Design of Road Pavements*; Austroads: Sydney, Australia, 2004.
39. Moghaddam, T.B.; Baaj, H. The use of rejuvenating agents in production of recycled hot mix asphalt: A systematic review. *Constr. Build. Mater.* **2016**, *114*, 805–816. [CrossRef]
40. Rahmadiawan, D.; Abral, H.; Yesa, W.H.; Handayani, D.; Sandrawati, N.; Sugiarti, E.; Ilyas, R.A. White Ginger Nanocellulose as Effective Reinforcement and Antimicrobial Polyvinyl Alcohol/ZnO Hybrid Biocomposite Films Additive for Food Packaging Applications. *J. Compos. Sci.* **2022**, *6*, 316. [CrossRef]
41. *AI 1991*; Thickness Design-Asphalt Pavements for Highways and Streets, Manual Series No.1. Asphalt Institute: Lexington, KY, USA, 1991.
42. Valdés, G.; Pérez-Jiménez, F.; Miró, R.; Martínez, A.; Botella, R. Experimental study of recycled asphalt mixtures with high percentages of reclaimed asphalt pavement (RAP). *Constr. Build. Mater.* **2011**, *25*, 1289–1297. [CrossRef]